Polarity-dependence of the defect formation in c-axis oriented ZnO by the irradiation of an 8 MeV proton beam

Kazuto Koike, Mitsuaki Yano, Shun-ichi Gonda, Akira Uedono, Shoji Ishibashi, Kazunobu Kojima, and Shigefusa F. Chichibu

Citation: Journal of Applied Physics **123**, 161562 (2018); doi: 10.1063/1.5010704
View online: https://doi.org/10.1063/1.5010704
View Table of Contents: http://aip.scitation.org/toc/jap/123/16
Published by the American Institute of Physics

Polarity-dependence of the defect formation in *c*-axis oriented ZnO by the irradiation of an 8 MeV proton beam

Kazuto Koike,[1,a)] Mitsuaki Yano,[1] Shun-ichi Gonda,[2] Akira Uedono,[3] Shoji Ishibashi,[4] Kazunobu Kojima,[5] and Shigefusa F. Chichibu[5]
[1]*Nanomaterials and Microdevices Research Center, Osaka Institute of Technology, Asahi-ku, Osaka 353-8585, Japan*
[2]*The Institute of Scientific and Industrial Research, Osaka University, Ibaraki, Osaka 567-0047, Japan*
[3]*Division of Applied Physics, Faculty of Pure and Applied Sciences, University of Tsukuba, Tsukuba, Ibaraki 305-8573, Japan*
[4]*Research Center for Computational Design of Advanced Functional Materials, National Institute of Advanced Industrial Science and Technology, Tsukuba, Ibaraki 305-8568, Japan*
[5]*Institute for Multidisciplinary Research for Advanced Materials, Tohoku University, Aoba-ku, Sendai 980-8577, Japan*

(Received 25 October 2017; accepted 22 December 2017; published online 10 January 2018)

The polarity dependence of the radiation hardness of single-crystalline ZnO bulk crystals is studied by irradiating the Zn-polar and O-polar *c*-planes with an 8 MeV proton beam up to the fluence of 4.2×10^{16} p/cm^2. To analyze the hardness, radiation-induced defects were evaluated using positron annihilation (PA) analysis, and the recovery by post-annealing was examined using continuous-wave photoluminescence (PL) and time-resolved photoluminescence (TRPL) measurements. It was suggested by the PA and PL analyses that the major defects in both polarities were $V_{Zn}V_O$ divacancies. While the PA data did not show the clear dependence on the polarity, the PL and TRPL results showed that the Zn-polar *c*-plane had a little higher radiation tolerance than that of the O-polar *c*-plane, which was consistent with the result that the increase in the electrical resistance by proton beam irradiation was smaller for the former one. Considering these results in total, the polarity dependence is considered to be not so large, but the Zn-polar *c*-plane has a little higher tolerance than that of the O-polar one. *Published by AIP Publishing.* https://doi.org/10.1063/1.5010704

I. INTRODUCTION

Wide bandgap semiconductor zinc oxide (ZnO) has been commonly used for electronic applications as varistors, piezoelectric transducers, transparent conducting films, and thin-film transistors (TFTs). Among them, ZnO-based TFTs are now opening newly developing application fields in printable electronics[1,2] and biosensors.[3] Furthermore, recent progress in epitaxial growth techniques enables us to apply ZnO to optoelectronic[4–6] and high-power[7,8] devices, promoting this material to be a potential candidate for novel applications in the next generation and gallium nitride (GaN).

In addition, ZnO has another advantage in radiation hardness which is of importance for device applications such as the electronics for space satellites and nuclear reactors; it has much higher radiation tolerance than that of GaN for the displacement damage (DD) effect. Since the tolerance to the DD effect[9] depends on the displacement threshold energy of constituent elements and hence increases with bandgap energy in general,[10,11] these two materials could be expected to have comparable tolerance due to the same wurtzite structure with nearly the same lattice constants and bandgap energies. The experimental results by many researchers, however, revealed that the tolerance of ZnO is one or two-orders of magnitude higher than that of GaN.

For instance, Look *et al*. studied the DD effect on ZnO single-crystals by irradiating the surface with 1–2 MeV electron beams and found much higher tolerance than that of Si, GaAs, CdS, and even GaN.[12,13] This outstandingly high tolerance of ZnO was also confirmed by Auret *et al*. by irradiating a 1.8 MeV proton beam,[14] Tuomisto *et al*. by irradiating a 2 MeV electron beam,[15,16] Zubiaga *et al*. by irradiating a 2 MeV O^+ ion beam,[17] and Koike *et al*. by irradiating an 8 MeV proton beam[18] and was explained by the high diffusivity of vacancies and interstitial atoms in ZnO, which promotes the self-repairing of radiation-induced defects.

Although many works have been reported for the radiation hardness of ZnO, little has been studied upon the polarity dependence, while the DD effect might be influenced by the polarity since the wurtzite structure lacks inversion symmetry along the *c*-axis direction as shown in Fig. 1. To our knowledge, only Look *et al*. studied the polarity dependence as discussed in Refs. 12 and 13 by measuring the degradation of electrical properties in vapor-transport grown ZnO bulk crystals with high electron mobility. They found that the O-polar (−) *c*-plane had a higher radiation hardness than that of the Zn-polar (+) *c*-polar one and explained the difference in terms of a multiple-displacement model.

In this paper, the polarity dependence of the DD effect on 8 MeV proton beam irradiation is studied for *c*-axis oriented ZnO bulk crystals by characterizing the defect-related properties using tools such as positron annihilation (PA), continuous-wave photoluminescence (PL), and time-resolved photoluminescence (TRPL). Different from Refs. 12 and 13, much popular ZnO bulk crystals grown by hydrothermal synthesis and a proton beam with large fluence were used to

[a)]Author to whom correspondence should be addressed: kazuto.koike@oit.ac.jp

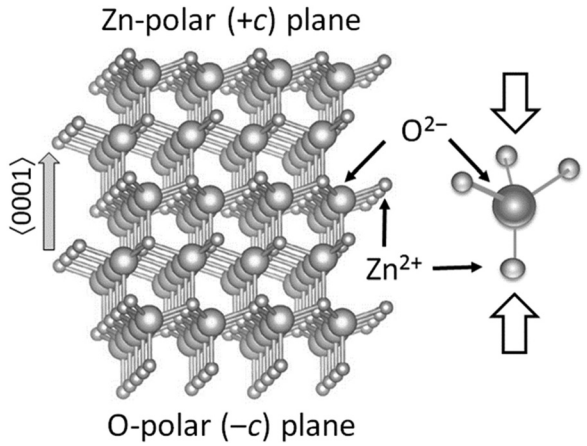

FIG. 1. Schematic cross-section of the atomic arrangement of ZnO. Arrows in the right figure show the direction of the proton beam irradiation studied in this experiment.

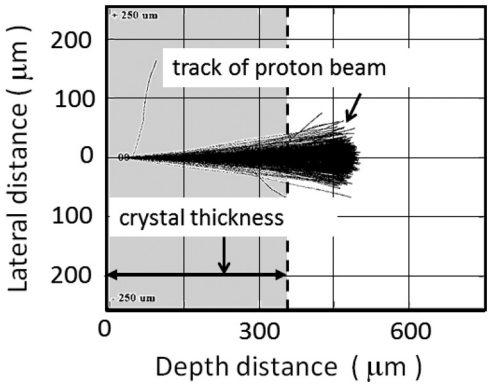

FIG. 2. Ion track trajectory output calculated by the SRIM code for the 8 MeV proton beam injected into ZnO. It is indicated that the proton beam passes through the 330-μm-thick ZnO crystals used in this experiment.

study the DD effect on higher crystallographic quality crystals under more severe irradiation conditions. The characterization was carried out by analyzing the PA data using a theoretical calculation of S and W parameters which represent the weights of the low- and high-momentum parts in annihilation spectra and by estimating the concentration of nonradiative recombination centers (NRCs) from the TRPL data.

II. EXPERIMENTAL PROCEDURE

The proton beam irradiation was carried out for the $+c$ and $-c$ planes of commercially available 330-μm-thick ZnO wafers that were sliced from a hydrothermally synthesized bulk single-crystal grown by Tokyo Denpa (TEW). The wafers were purchased in 2012 after annealing at 1400 °C to remove Li impurities and subsequent mirror-polishing. For these $+c$ and $-c$ samples, the full-width at half-maximum (FWHM) of the 0004 reflection locking curve of X-ray diffraction (XRD) was measured as around 80 arcsec by using our Rigaku-made SmartLab XRD system. This value was roughly one-fourth of the FWHM measured by the same system for a vapor-transport grown ZnO bulk crystal purchased from Eagle Pitcher, indicating the higher crystallographic quality of the hydrothermally synthesized crystals. The conductivity type of these samples was n-type, and the electron concentration before the irradiation was around $6 \times 10^{14}\,\mathrm{cm}^{-3}$ for the $+c$ sample and around $1 \times 10^{15}\,\mathrm{cm}^{-3}$ for the $-c$ one with nearly the same electron mobility of approximately $130\,\mathrm{cm}^2/\mathrm{Vs}$ at room temperature.

These two samples were set side by side on a thermo-controlled sample holder kept at around 0 °C in an irradiation vacuum chamber and simultaneously irradiated perpendicular to the surfaces by an 8 MeV proton beam with a rate of about $9 \times 10^{11}\,\mathrm{p/cm}^2\,\mathrm{s}$ from a tandem-type accelerator equipped at The Wakasawan Energy Research Center.[19] Under the above-mentioned condition, the proton beam is expected to pass through the ZnO crystals since the ion track trajectory output calculated for semi-infinite long ZnO by the SRIM code[20] reaches around 420 μm as shown in Fig. 2. It is noteworthy that specific atomic arrangement was not considered for the calculation.

During the proton beam irradiation, we measured the change in the electrical resistance of the samples using a two-terminal method to monitor the progression of radiation damage. After the irradiation, the samples were taken out of the irradiation chamber and kept in a protection box for roughly 6 months to wait for the cooling down of radioactivation.

To the samples after the cooling down period, XRD was measured first although no significant change was observed; the crystallographic quality was found to be scarcely affected by the proton beam irradiation within the purview of the XRD rocking curves of symmetric and asymmetric reflections and reflection angles. Then, the radiation-induced defect states were characterized using a PA technique by evaluating the Doppler broadening of $m_0c^2 = 511\,\mathrm{keV}$ annihilation γ rays ($E_\gamma = m_0c^2 \pm \Delta E_\gamma$, where m_0 is the mass of a positron, c is the velocity of light, and ΔE_γ is the Doppler broadening) at room temperature.[21] The Doppler broadening of the radiation spectra was measured with a Ge detector as a function of incident positron energy. For each incident positron energy, a spectrum with about 3×10^6 counts was obtained, and the resultant spectra were analyzed by defining the parameters S and W as $\Delta E_\gamma \leq 0.76\,\mathrm{keV}$ and $3.4\,\mathrm{keV} \leq \Delta E_\gamma \leq 6.8\,\mathrm{keV}$, respectively.[22]

After the PA measurement, each sample was sequentially annealed for 10 min at every 200 °C step in an oxygen atmosphere by measuring repeatedly their PL and TRPL spectra. The annealing was conducted by sandwiching the sample with protective ZnO wafers using rapid thermal annealing equipment at a heating/cooling rate of 1 °C/s, and the annealing period of 10 min was chosen by taking practical experimental conditions into account. The PL measurement was conducted at 10 and 300 K using a $5\,\mathrm{W/cm}^2$ He-Cd ion laser for excitation. The TRPL measurement was carried out at 300 K to quantify the nonradiative recombination lifetime of minority carriers (τ_{NR}), using a frequency-tripled mode-locked Al_2O_3:Ti laser as an excitation source.[23,24] The excitation power density was set at $120\,\mathrm{nJ/cm}^2$ per pulse to ensure the weak excitation conditions, and a standard streak-camera was used for the signal acquisition.

III. RESULTS AND DISCUSSION

Figure 3 shows the *in-situ* monitored change in the electrical resistance of the samples during proton beam irradiation. The irradiation was conducted up to 4.2×10^{16} p/cm^2. The vertical axis represents the electrical resistance, and the horizontal axis represents the fluence of the proton beam. Indeed, the resistance change measured by the two-terminal method contains the contribution from contact resistance and hence does not directly correspond to the resistivity change in the bulk crystals, but we monitored it as a rough estimation of the radiation damage.

Actually, we observed a gradual decrease in the resistance after loading the samples into the vacuum chamber, which was presumably due to the decrease in contact resistance via the reduction of the depletion layer by the desorption of OH^- species from the surface.[25] On the other hand, the rapid increase in the higher fluence region in Fig. 3 could be related to the formation of radiation-induced defects that may decrease the concentration and mobility of conduction electrons.[18] In fact, both $+c$ and $-c$ samples in this region gradually changed their color from clear transparent to yellowish transparent with the progress of the irradiation period, presumably due to the formation of defect-related deep levels in the bandgap energy. As seen in Fig. 3, the rapid increase in the electrical resistance of the $+c$ sample starts at the higher fluence compared with that of the $-c$ one, suggesting that the $+c$ plane has higher radiation hardness than that of the $-c$ one.

To the samples before and after the proton beam irradiation with the fluence of 4.2×10^{16} p/cm^2, the S parameters in PA were analyzed as a function of positron acceleration energy E. The resultant data are shown in Fig. 4, where the mean implantation depth of positrons is given in the upper horizontal axis. The rapid increase in S in the low energy region is due to the annihilation of positrons with positronium atoms at the surface, and the slope of this region reflects the positron diffusion length L_d. At $E > 15$ keV, on the other hand, S begins to have a constant value S_b by representing the characteristics of bulk states. The values of these L_d and S_b for both samples were roughly 50 nm and 0.424 before irradiation and 10 nm and 0.440 after irradiation,

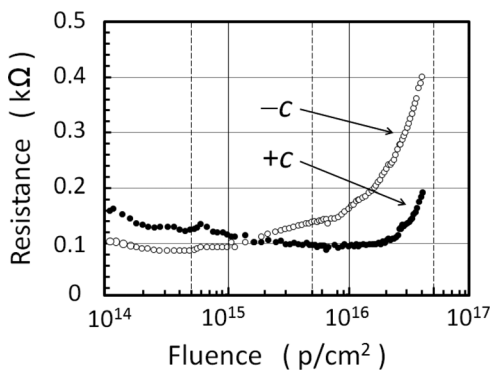

FIG. 3. *In-situ* monitored change in the two-terminal electrical resistance of the ZnO samples during irradiation. Solid and open plots represent the resistance of the $+c$ and $-c$ ZnO samples, respectively.

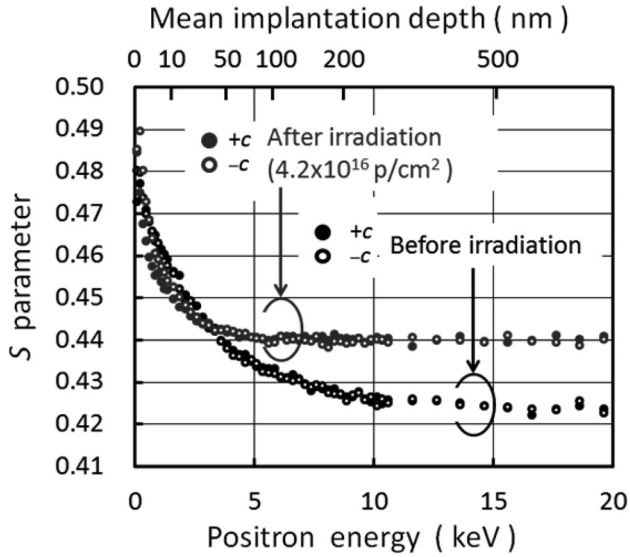

FIG. 4. *S*-*E* relationship of the PA data measured for the ZnO samples before and after the 8 MeV proton beam irradiation with the fluence of 4.2×10^{16} p/cm^2. Solid and open plots represent the signals form the $+c$ and $-c$ ZnO samples, respectively.

respectively. Because positrons are trapped at neither interstitials nor positively charged defects such as oxygen vacancies, V_O, the observed changes in S_b and L_d were attributed to the trapping of positrons by Zn vacancies, V_{Zn}, and/or complex vacancies between V_{Zn} and V_O.[23,24,26] Accordingly, the increase in S_b and the decrease in L_d indicate the increase in the size and/or concentration of those negatively charged vacancies in the ZnO crystals after proton beam irradiation.

From the viewpoint of the polarity dependence, on another front, one can see no significant difference in S_b and L_d between the $+c$ and $-c$ samples despite the expectation from the data on electrical resistance shown in Fig. 3. This discrepancy might be due to the very high fluence of the proton beam used in this experiment; we are afraid of the possibility that the polarity dependence in PA has been shielded by the large amount of the defects formed at this severely damaged stage.

In order to characterize the defect type more precisely in the next step, the *S*-*W* relationship of the PA data was analyzed as shown in Fig. 5, where the (S,W) values denoted by solid and open symbols represent the theoretical and experimental results, respectively. In the theoretical calculation, annihilation parameters were estimated for the positrons at the delocalized state free from defects "bulk," the positrons trapped at "V_{Zn}," divacancy "$V_{Zn}V_O$," and larger vacancy complexes "$V_{Zn}(V_O)_2$" and "$(V_{Zn}V_O)_2$," using the valence-electron wave functions determined by a projector augmented-wave method.[27,28] As shown in Fig. 5, the (S,W)-value calculated for "bulk" ZnO locates at a little lower left of the experimental result for ZnO before irradiation. This difference might be due to the limitation of the theoretical calculation applied to the Doppler broadening spectra, temperature dependent differences between the modeling and experimental conditions, the experimental background, and/or the energy resolution of the detector used for the measurement of annihilation radiation.

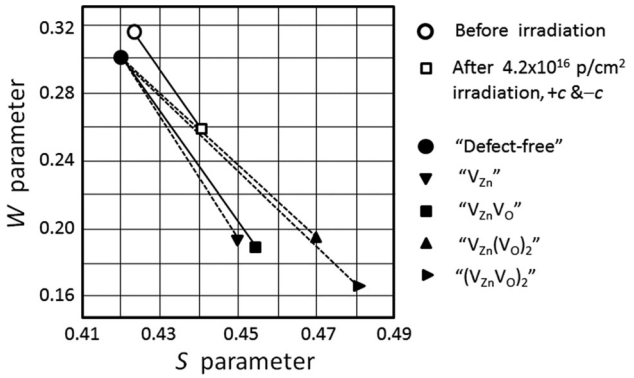

FIG. 5. *S*-*W* relationship of the defects in ZnO. Open and solid plots are experimental data and their theoretical calculation, respectively. The experimental data for the $+c$ and $-c$ ZnO samples after irradiation were nearly overlapped in the presented scale.

Considering the slope of the (*S*,*W*)-shift, both V_{Zn} and $V_{Zn}V_O$ can be probable candidates for the vacancies generated by the severe proton beam irradiation. We estimate the proper candidate to be $V_{Zn}V_O$ since the slope of the experimental data in Fig. 5 is just consistent with that of the theoretical one from the "bulk" to "$V_{Zn}V_O$," and the PL properties after irradiation are consistent with the characteristics of $V_{Zn}V_O$ as discussed in the following paragraph. It should be mentioned that the present theoretical results of *S* and *W* parameters are in good agreement with those reported in a preceding work[29] although stringent comparison is difficult because the definitions of these parameters are different in detail.

The PL spectra observed from the samples before and after proton beam irradiation are shown in Figs. 6(a)–6(d). Roughly speaking, each spectrum at 10 and 300 K from the sample after irradiation, Figs. 6(c) and 6(d), respectively,

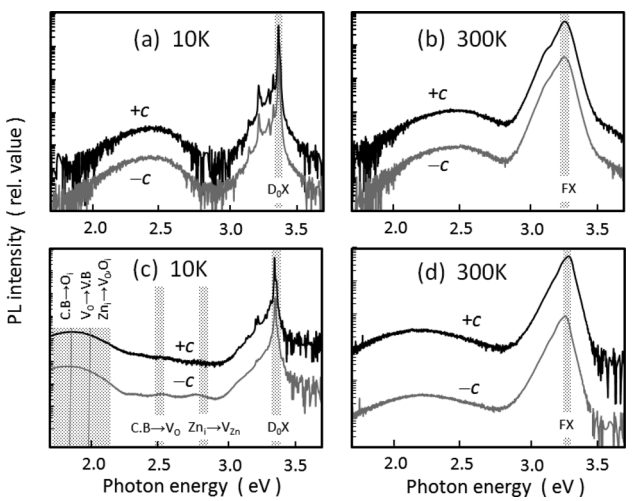

FIG. 6. PL spectra measured from the $+c$ and $-c$ ZnO samples before and after irradiation. (a) and (b) The PL spectra measured at 10 and 300 K from the samples before irradiation, respectively. (c) and (d) The PL spectra measured at 10 and 300 K from the samples after irradiation, respectively. The vertical axis represents the relative PL intensity in logarithmic scale, and the spectra are normalized by their NBE peak intensity and depicted by shifting the $+c$ spectrum about an order of magnitude higher in intensity from the $-c$ one. It should be noted that the emission intensity from the samples after irradiation was roughly one-thousandth of that from the samples before irradiation. The transitions assigned from literatures (Refs. 25–27) to respective emission bands are given in the figures.

showed nearly the same shapes as that from the sample before irradiation, Figs. 6(a) and 6(b), respectively, except for the much smaller intensity of about one-thousandth and the red-shift of the small and broad emission peak in the visible region from the green band to the yellow one (at 300 K) or to the red one (at 10 K). This dramatic decrease in intensity throughout the spectra should indicate that the major vacancy formed by the proton beam irradiation is $V_{Zn}V_O$ because this type of divacancy in ZnO is known to act as NRC,[23,24,30] while V_{Zn} in ZnO forms a radiative recombination center.[23,24,30–32]

The most intense near-band edge (NBE) emission peak at 10 K in Figs. 6(a) and 6(c) locates at around 3.36 eV which is due to the recombination process of the A-excitons bound to neutral donors.[31] On the other hand, the most intense NBE emission peak at 300 K in Figs. 6(b) and 6(d) locates at around 3.28 eV which is presumably due to the recombination process of free A-excitons mixed with that of the free B-excitons coupled with 1 LO-phonon replica.[31]

In the spectra at 10 K shown in Fig. 6(c), the small and broad emission peak in the red band of the $+c$ and $-c$ samples might be due to the transitions related to defect-induced deep levels such as those from the conduction band (C.B) to interstitial oxygens, O_i (2.0–1.8 eV),[32,33] from V_O to the valence band (V.B) (1.8–1.65 eV),[32,33] and from interstitial Zn, Zn_i, to V_O and O_i (2.25–2.0 eV).[33] Other much smaller sub-peaks appeared in the yellow band of the $-c$ sample might be related to the transitions from Zn_i to V_{Zn} (*ca*, 2.8 eV)[33] and from the C.B to V_O (*ca*, 2.5 eV).[33] At 300 K, these defect-related peaks merged into a single broad emission band in the visible region as shown in Fig. 6(d).

Then, these damaged samples were sequentially annealed in an O_2 atmosphere for 10 min at every 200 °C step to study the recovery steps of defects. In Figs. 7(a) and 7(b), the PL spectra at 10 and 300 K are shown for the samples after annealing at 600 °C, respectively, as the representative data of annealed samples. Compared with the corresponding spectra in Figs. 6(a)–6(d), the major part of the respective spectra is roughly close to each other although there is a little difference in the visible band emission, i.e., neither the selective increase in specific peaks nor the development of new peaks was notably observed throughout the annealing experiment up to 800 °C.

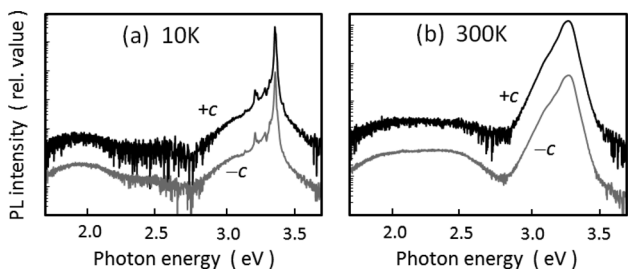

FIG. 7. PL spectra measured from the irradiated $+c$ and $-c$ ZnO samples after annealing at 600 °C. (a) and (b) The PL spectra measured at 10 and 300 K, respectively. The vertical axis represents the relative PL intensity in logarithmic scale, and the spectra are normalized by their NBE peak intensity and depicted by shifting the $+c$ spectrum about an order of magnitude higher in intensity from the $-c$ one.

The intensity change in the NBE emission peak at 10 and 300 K is summarized in Fig. 8 as a function of annealing temperature, where the vertical axis represents the relative value to the respective intensities before irradiation. One can see that the degree of the degradation in the PL at 300 K was more than two-orders of magnitude larger than that in the PL at 10 K, which leads to much faster recovery of the PL intensity at 10 K. Furthermore, the small but clear difference in the degradation rate between the $+c$ and $-c$ samples at low annealing temperatures might indicate a little higher radiation tolerance of the former one. It is also seen that the recovery of the PL intensity at 300 and 10 K became obvious after annealing above 400 °C, which was associated with a gradual breaching of the appearance of the $+c$ and $-c$ samples with the increase in annealing temperature above 400 °C by recovering the initial clear transparency at 800 °C.

These recovery steps were also analyzed for the annealed samples by measuring the TRPL response of the NBE emission peak at 300 K. The PL lifetime (τ_{PL}), which represents the inverse of the minority carrier (or exciton) recombination rate (R), is the inverse sum of the radiative and nonradiative recombination rates (R_R and R_{NR}, respectively, which are the inverse of respective recombination lifetimes, τ_R and τ_{NR}). As R_R decreases with temperature due to the increase in the kinetic energy term, room temperature τ_{PL} of defective and most of the standard quality bulk semiconductor materials is dominated by τ_{NR}. Therefore, τ_{PL} increases as the quality is improved.[23,24,34]

As shown by the representative data in Fig. 9 for the samples after annealing at 600 °C, each TRPL response from the $+c$ and $-c$ samples exhibited a bi-exponential decay shape with a form of $I(t) = A_1\exp(-t/\tau_1) + A_2\exp(-t/\tau_2)$, where $I(t)$ is the intensity at time t and A_1 (A_2) and τ_1 (τ_2) are the pre-exponential factor and decay time for the fast (slow) decay component, respectively. Such a bi-exponential decay response appears to agree with the previous reports on ZnO,[34,35] and we ascribed our degraded τ_1 and τ_2 values to τ_{NR} in more and less seriously damaged regions, respectively. Compared with the values reported for high quality bulk ZnO crystals being $\tau_1 \sim 200$ ps and $\tau_2 \sim 1$ ns,[23,24,26,31,34] the lifetimes at this annealing step were largely degraded as yet; $\tau_1 = 127$ ps and $\tau_2 = 310$ ps for the $-c$ sample and $\tau_1 = 130$ ps and $\tau_2 = 340$ ps for the $+c$ sample.

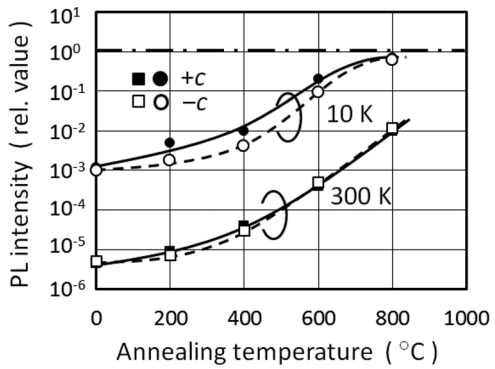

FIG. 8. Intensity change in the NBE emission in the PL spectra from the ZnO samples after annealing. Solid and open plots represent the signals form the $+c$ and $-c$ samples, respectively.

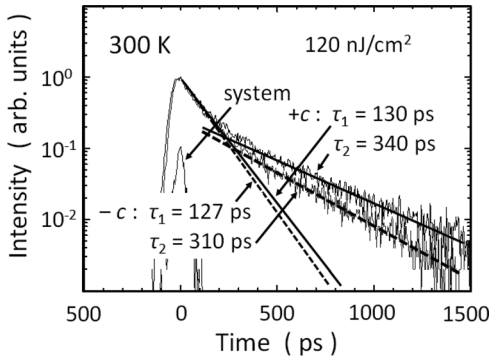

FIG. 9. Intensity response of the NBE emission at 300 K measured by TRPL from the $+c$ and $-c$ ZnO samples after 600 °C annealing. Solid and dashed lines show the decay components of the $+c$ and $-c$ ZnO samples with the corresponding time-constants, respectively.

The TRPL data after annealing are summarized in Fig. 10 as a function of reciprocal annealing temperature T_a. One can see a clear difference in the defect-recovery steps between the $+c$ and $-c$ samples; both τ_1 and τ_2 at $T_a < 400$ °C were longer for the $+c$ sample than those for the $-c$ one although those of the latter sample recovered faster and became nearly the same as those of the former one at $T_a \geq 400$ °C. Thus, larger degradation in τ_1 and τ_2 is expected for the $-c$ sample before annealing, which may indicate the lower radiation hardness of the $-c$ plane compared with that of the $+c$ one.

One can estimate the concentration of NRCs (N_{NRC}) from the TRPL data using the relationship between τ_1 and N_{NRC} given in Fig. 3 of a previous study.[36] N_{NRC} is roughly estimated for the irradiated samples after the annealing at 200 and 600 °C with the τ_1 values shown in Fig. 10 and

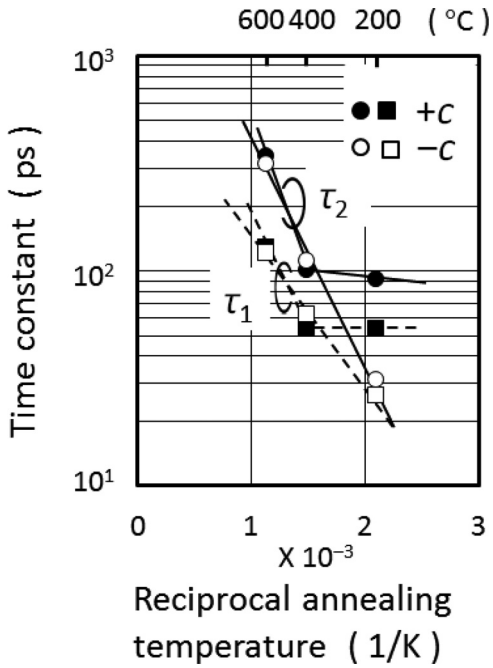

FIG. 10. Time-constants of the decay curves in TRPL data from the $+c$ and $-c$ ZnO samples as a function of reciprocal annealing temperature. Solid and open plots represent the signals from the $+c$ and $-c$ samples, respectively. Square and circle plots represent the fast ($\tau 1$) and the slow ($\tau 2$) decay components in the TRPL spectra, respectively.

obtained to be the latter half of the order of $10^{17}\,cm^{-3}$ and approximately $1 \times 10^{17}\,cm^{-3}$, respectively, by ignoring the small difference between the $+c$ and $-c$ samples. Since the value for high quality bulk crystals ($\tau_1 \sim 200$ ps) is expected as the latter half of the order of $10^{16}\,cm^{-3}$, this monotonous decrease in N_{NRC} should directly indicate the progress of defect recovery with the increase in annealing temperature. Furthermore, it is also shown by Fig. 10 that the annealing at around 900 °C will recover the defect states in both samples close to their initial levels by extrapolating the Arrhenius plot.

Considering these experimental data shown in Figs. 3–10 in total, one might be able to conclude that the difference in the tolerance to the DD effect is small but a little higher for the $+c$ plane than that for the $-c$ one from the viewpoint of PL efficiency although further analysis should be done by irradiating ZnO samples with much smaller fluence of the orders of 10^{14}–10^{15} p/cm^2. This observed polarity dependence, however, is contrary to the reported one by Look *et al.*,[12,13] where $-c$ plane ZnO had higher radiation hardness than that of the $+c$ one for the electrical properties under the 2 MeV electron beam irradiation up to 4×10^{16} e/cm^2. It is not clearly understood the account at present yet, this discrepancy might be due to the difference in evaluation criteria and/or the degree of degradation; the DD effect of our study is estimated to be roughly 200 times harder than the case of Look *et al.* by taking the difference of non-ionizing energy loss (NIEL) factors expected for the protons at 8 MeV and the electrons at 2 MeV into account.[9,37]

We previously reported on GaN that the Ga-polar ($+c$) plane had a little higher radiation hardness than that of the N-polar ($-c$) one under the same 8 MeV proton beam irradiation.[38] Therefore, our experimental results for ZnO and GaN indicate that the radiation hardness becomes high when the incident proton beam is irradiated to their $+c$ planes. For ZnO and GaN, the displacement threshold energies for cation and anion atoms are reported as follows: $E_d(Zn) = 18.5$ eV and $E_d(O) = 41.4$ eV for ZnO[39] and $E_d(Ga) = 45$ eV on average (18 eV in minimal) and $E_d(N) = 109$ eV on average (22 eV in minimal) for GaN.[40] As shown in Fig. 1, each cation atoms in the $+c$-axis direction is bonded to the right upper anion atoms. Therefore, the cation atoms with smaller E_d are protected from the direct bombardment of the proton beam by the anion atoms with larger E_d when the proton beam is irradiated to the $+c$ planes, and the situation is reversible for the proton beam irradiation to the $-c$ planes. This difference in the shadow-cone effect might be responsible for the slightly higher irradiation hardness of the $+c$ plane ZnO compared to that of the $-c$ one.

IV. SUMMARY

We experimentally examined the polarity dependence of the radiation hardness on ZnO bulk crystals by irradiating an 8 MeV proton beam to the $+c$ and $-c$ planes. The analysis by PA showed a negligible difference for these two configurations. The analysis by PL and TRPL, on the other hand, indicated a little higher radiation hardness of the $+c$ plane although the difference was not large. Considering these experimental data in total, we conclude that the difference in the tolerance to the DD effect on PL properties under the severe proton beam irradiation is small but a little higher for the $+c$ plane than that of the $-c$ one. The PA, PL, and TRPL analyses confirmed that the major radiation-induced defects are $V_{Zn}V_O$ divacancies, which act as NRC, and the defects are obviously recovered after annealing over 400 °C by reaching the initial quality before irradiation after annealing at around 900 °C.

ACKNOWLEDGMENTS

The authors wish to thank Dr. R. Ishigami and Dr. K. Kume at The Wakasawan Energy Research Center for the professional help with the proton beam irradiation and T. Ohtomo at Tohoku University for the attentive help with the optical measurement. This work was supported in part by the "Network Joint Research Center for Materials and Devices" by MEXT and by JSPS KAKENHI Grant Nos. JP25390033 and JP16K04936.

[1]X. Liu, L. Gu, Q. Zhang, J. Wu, Y. Long, and Z. Fan, Nat. Commun. **5**, 4007 (2014).
[2]Y. Kimura, Y. Sun, T. Maemoto, S. Sasa, S. Kasai, and M. Inoue, Jpn. J. Appl. Phys. **52**, 06GE09 (2013).
[3]M. Yano, K. Koike, K. Mukai, T. Onaka, Y. Hirofuji, K. Ogata, S. Omatu, T. Maemoto, and S. Sasa, Phys. Status Soldi A **211**, 2098 (2014).
[4]K. Koike, K. Hama, I. Nakajima, G. Takada, K. Ogata, S. Sasa, M. Inoue, and M. Yano, J. Cryst. Growth **278**, 288 (2005).
[5]A. Tsukazaki, A. Ohtomo, T. Onuma, M. Ohtani, T. Makino, M. Sumiya, K. Ohtani, S. F. Chichibu, S. Fuke, Y. Segawa, H. Ohno, H. Koinuma, and M. Kawasaki, Nat. Mater. **4**, 42 (2005).
[6]K. Nakahara, S. Akasaka, H. Yuji, K. Tamura, T. Fujii, Y. Nishimoto, D. Takamizu, A. Sasaki, T. Tanabe, H. Takasu, H. Amaike, T. Onuma, S. F. Chichibu, A. Tsukazaki, A. Ohtomo, and M. Kawasaki, Appl. Phys. Lett. **97**, 013501 (2010).
[7]S. Sasa, M. Ozaki, K. Koike, M. Yano, and M. Inoue, Appl. Phys. Lett. **89**, 053502 (2006).
[8]H. Arabshahi, Mod. Phys. Lett. B **23**, 2533 (2009).
[9]G. P. Summers, E. A. Burke, P. Shapiro, S. R. Messenger, and R. J. Walters, IEEE Trans. Nucl. Sci. **40**, 1372 (1993).
[10]A. L. Barry, B. Lchmann, D. Fritsch, and D. Bräunig, IEEE Trans. Nucl. Sci. **38**, 1111 (1991).
[11]A. I. Nedelcescu, C. Carlone, A. Houdayer, H. J. von Bardeleben, J. L. Cantin, and S. Raymond, IEEE Trans. Nucl. Sci. **49**, 2733 (2002).
[12]D. C. Look, D. C. Reynolds, J. W. Hemsky, R. L. Jones, and J. R. Sizelove, Appl. Phys. Lett. **75**, 811 (1999).
[13]D. C. Look, J. W. Hemsky, and J. R. Sizelove, Phys. Rev. Lett. **82**, 2552 (1999).
[14]F. D. Auret, S. A. Goodman, M. Hayes, M. J. Legodi, H. A. van Laarhoven, and D. C. Look, Appl. Phys. Lett. **79**, 3074 (2001).
[15]F. Tuomisto, V. Ranki, K. Saarinen, and D. C. Look, Phys. Rev. Lett. **91**, 205502 (2003).
[16]F. Tuomisto, D. C. Look, and G. C. Farlow, Physica B **401/402**, 604 (2007).
[17]A. Zubiaga, F. Tuomisto, V. A. Coleman, H. H. Tan, C. Jagadish, K. Koike, S. Sasa, M. Inoue, and M. Yano, Phys. Rev. B **78**, 035125 (2008).
[18]K. Koike, T. Aoki, R. Fujimoto, S. Sasa, M. Yano, S. Gonda, R. Ishigami, and K. Kume, Phys. Status Solidi C **9**, 1577 (2012).
[19]See http://www.werc.or.jp/ for The Wakasawan Energy Research Center.
[20]See http://www.srim.org/ for SRIM simulation.
[21]A. Uedono, T. Koida, A. Tsukazaki, M. Kawasaki, Z. Q. Chen, S. F. Chichibu, and H. Koinuma, J. Appl. Phys. **93**, 2481 (2003).
[22]A. Uedono, S. Ishibashi, K. Tenjinbayashi, T. Tsutsui, K. Nakahara, D. Takamizu, and S. F. Chichibu, J. Appl. Phys. **111**, 014508 (2012).
[23]S. F. Chichibu, A. Uedono, A. Tsukasaki, T. Onuma, M. Zamfirescu, A. Ohtomo, A. Kavokin, G. Cantwell, C. W. Litton, T. Sota, and M. Kawasaki, Semicond. Sci. Technol. **20**, S67 (2005).

[24]S. F. Chichibu, T. Onuma, M. Kubota, A. Uedono, T. Sota, A. Tsukazaki, A. Ohtomo, and M. Kawasaki, J. Appl. Phys. **99**, 093505 (2006).
[25]K. Ogata, K. Koike, Y. Hirata, S. Sasa, M. Inoue, and M. Yano, J. Soc. Mater. Sci. Jpn. **55**, 159 (2006).
[26]T. Koida, S. F. Chichibu, A. Uedono, A. Tsukazaki, M. Kawasaki, T. Sato, Y. Segawa, and H. Koinuma, Appl. Phys. Lett. **82**, 532 (2003).
[27]S. Ishibashi, Mater. Sci. Forum **445/446**, 401 (2004).
[28]See http://qmas.jp/ for QMAS (Quantum MAterials Simulator).
[29]I. Makkonen, E. Korhonen, V. Prozheeva, and F. Tuomisto, J. Phys.: Condens. Matter **28**, 224002 (2016).
[30]Z. Q. Chen, K. Betsuyaku, and A. Kawasuso, Phys. Rev. B **77**, 113204 (2008).
[31]A. Teke, Ü. Özgür, S. Doğan, X. Gu, H. Morkoç, B. Nemeth, J. Nause, and H. O. Everitt, Phys. Rev. B **70**, 195207 (2004).
[32]B. Cao, W. Cai, and H. Zeng, Appl. Phys. Lett. **88**, 161101 (2006).
[33]N. H. Alvi, K. ul Hasan, O. Nur, and M. Willander, Nanoscale Res. Lett. **6**, 130 (2011).
[34]Ü. Özgür, Y. I. Alivov, C. Liu, A. Teke, M. A. Reshchikov, S. Doğan, V. Avrutin, S.-J. Cao, and H. Morkoç, J. Appl. Phys. **98**, 041301 (2005).
[35]D. C. Reynolds, D. C. Look, B. Jogai, J. E. Hoelscher, R. E. Sherriff, M. T. Harris, and M. J. Callahan, J. Appl. Phys. **88**, 2152 (2000).
[36]S. F. Chichibu, K. Kojima, Y. Yamazaki, K. Furusawa, and A. Uedono, Appl. Phys. Lett. **108**, 021904 (2016).
[37]K. Koike, R. Fujimoto, R. Wada, S. Sasa, M. Yano, S. Gonda, R. Ishigami, and K. Kume, Mater. Res. Symp. Proc. **1432**, 159 (2012).
[38]M. Matsuo, T. Murayama, K. Koike, S. Sasa, M. Yano, S. Gonda, A. Uedono, R. Ishigami, K. Kume, T. Ohtomo, E. Furukawa, Y. Yamazaki, K. Kojima, and S. Chichibu, in *Proceedings of the IEEE IMFEDK2015* (2015), p. 50.
[39]J. A. Van Vechten, in *Handbook on Semiconductors*, edited by T. S. Moss and S. P. Keller (North-Holland, Amsterdam, 1980), Chap. 1.
[40]S. J. Pearton, R. Deist, F. Ren, L. Liu, A. Y. Polyakov, and J. Kim, J. Vac. Sci. Technol., A **31**, 050801 (2013).